NANO LETTERS

pubs.acs.org/NanoLett

Letter

DNA Anchoring Strength Directly Correlates with Spherical Nucleic Acid–Based HPV E7 Cancer Vaccine Potency

Jeongmin Hwang,[‖] Jasper Wilson Dittmar,[‖] Janice Kang, Tonatiuh Ocampo, Michael Evangelopoulos, Zhenyu Han, Sergej Kudruk, Jochen Lorch,* and Chad A. Mirkin*

Cite This: *Nano Lett.* 2024, 24, 7629–7636

Read Online

ACCESS | Metrics & More | Article Recommendations | Supporting Information

ABSTRACT: Vaccination for cancers arising from human papillomavirus (HPV) infection holds immense potential, yet clinical success has been elusive. Herein, we describe vaccination studies involving spherical nucleic acids (SNAs) incorporating a CpG adjuvant and a peptide antigen ($E7_{11-19}$) from the HPV-E7 oncoprotein. Administering the vaccine to humanized mice induced immunity-dependent on the oligonucleotide anchor chemistry (cholesterol vs $(C12)_9$). SNAs containing a $(C12)_9$-anchor enhanced IFN-γ production >200-fold, doubled memory $CD8^+$ T-cell formation, and delivered more than twice the amount of oligonucleotide to lymph nodes *in vivo* compared to a simple admixture. Importantly, the analogous construct with a weaker cholesterol anchor performed similar to admix. Moreover, $(C12)_9$-SNAs activated 50% more dendritic cells and generated T-cells cytotoxic toward an HPV^+ cancer cell line, UM-SCC-104, with near 2-fold greater efficiency. These observations highlight the pivotal role of structural design, and specifically oligonucleotide anchoring strength (which correlates with overall construct stability), in developing efficacious therapeutic vaccines.

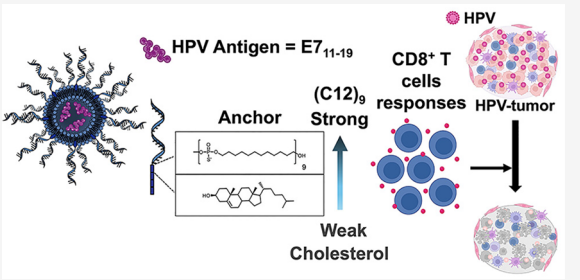

KEYWORDS: *spherical nucleic acids, immunotherapeutic vaccine, Toll-like receptor agonist, HPV-associated cancers*

Persistent infection with high-risk HPV is the leading cause of several cancers affecting more than 45,000 new patients annually in the US alone.[1] Despite the development of successful prophylactic vaccines, the incidence of HPV-associated cancers continues to rise.[2] During HPV infection, the HPV E6 and E7 viral oncoproteins disrupt the activity of cellular tumor suppressor proteins leading to tumorigenesis.[3] The tumor-specific expression of these oncoproteins provides several antigenic targets for immunotherapeutic treatments. Namely, a phase I clinical trial utilizing T cell receptor therapy (TCR-T) with T cells engineered to target the HPV $E7_{11-19}$ antigen demonstrated robust tumor regression with objective responses to therapy in 6 of 12 patients with metastatic HPV-associated cancers.[4] The high-avidity $E7_{11-19}$ human leukocyte antigen serotype A2 (HLA-A*02) complex-targeting showed promising antitumor effector functions such as interferon-gamma (IFN-γ) production and tumor cytolysis. However, TCR-T cell therapy often faces challenges due to toxicity caused by off-target effects, resistance mechanisms, and accessibility.[5] To overcome these challenges, therapeutic vaccine approaches were explored, incorporating the HPV $E7_{11-19}$ peptide with a toll-like receptor (TLR) agonist in an oil depot, then examined in clinical trials.[6,7] However, that approach has faced limitations and poor clinical success due to its inability to produce sufficient quantities of antigen-specific T cells.[6,7] The clinical effectiveness of T cells targeting the $E7_{11-19}$ antigen in TCR-T approaches[4] presents an ideal scenario to test whether advances made in therapeutic cancer vaccination by structuring vaccine components can demonstrate improved delivery of those components to specific immune cells and maximize the potency of the high-avidity $E7_{11-19}$-HLA complex for antitumor efficacy.

Spherical nucleic acid (SNA) constructs are a therapeutic platform[8−12] that have been used as vaccines to upregulate the activity of clinically relevant antigens through structural control of the vaccine's components.[13,14] SNAs are comprised of a nanoparticle core with radially oriented DNA on the surface which confers advantageous biological properties to both the DNA and the nanoparticle.[8] SNAs comprised of a liposome core with TLR-9 agonist CpG-motif DNA and peptide antigens readily internalize into antigen presenting cells (APCs), such as dendritic cells (DCs), leading to effective T cell priming.[10,15] These immune activities are highly dependent on the structural features of SNAs including antigen location,[16,17] antigen attachment chemistry,[18,19] and nano-

Received: March 22, 2024
Revised: June 5, 2024
Accepted: June 7, 2024
Published: June 14, 2024

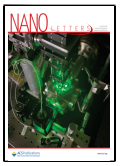

https://doi.org/10.1021/acs.nanolett.4c01392
Nano Lett. 2024, 24, 7629−7636

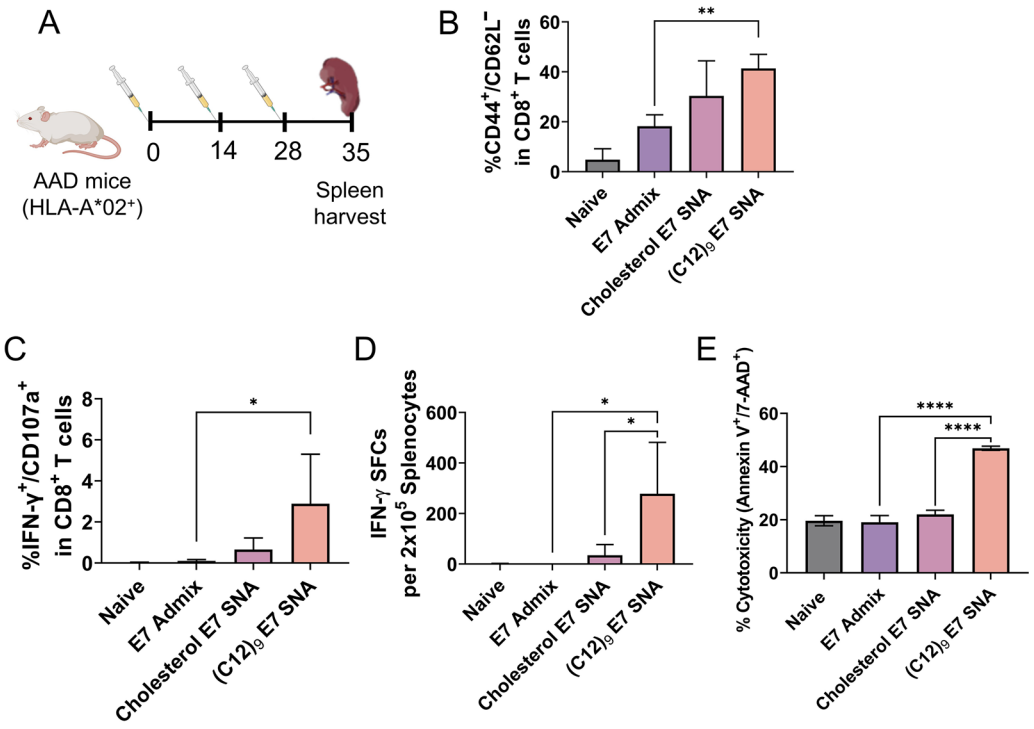

Figure 1. Vaccination of AAD mice with SNAs formulated with $E7_{11-19}$ antigen. A. Injection timeline for vaccination. B. Effector memory phenotype ($CD44^+$ and $CD62L^-$) within $CD8^+$ T cells. C. Intracellular IFN-γ levels ($CD107a^+$ and IFN-γ^+) in $CD8^+$ T cells following a 4 h restimulation with $E7_{11-19}$ antigen. D. IFN-γ secretion by splenocytes using ELISpot assay 48 h after restimulation ex vivo with $E7_{11-19}$ antigen. E. Antigen-specific killing by splenic $CD8^+$ cytotoxic T lymphocytes raised from vaccination against $E7_{11-19}$ pulsed T2 cells. Data represents mean ± standard deviation with $n = 5$ for panels B,C,D, $n = 3$ for panel E; statistical significance was calculated by one-way ANOVA with Tukey's post hoc test among the treatment groups; $^*P < 0.05$, $^{**}P < 0.01$, $^{***}P < 0.005$, and $^{****}P < 0.001$.

particle stability.[20,21] Specifically, the stability of liposomal SNAs plays a crucial role in improving vaccine function, with recent efforts focused on modifying the composition of the lipid bilayer and the lipophilic anchor that tethers the oligonucleotide to the liposome. Prior to this work, we chemically attached dodecane oligomers (C12, $n = 4-10$) to the TLR-9 CpG adjuvant DNA to optimize the stability and potency of immunostimulatory liposomal SNAs, ultimately finding that 9-C12 units ($(C12)_9$ SNAs) resulted in the most stable and potent constructs.[22] In comparison with conventional cholesterol-anchored SNAs, $(C12)_9$-anchored SNAs resulted in a 4-fold increase in serum half-life of the DNA shell, a 4-fold enhancement in immunostimulation, and a 6-fold enhancement in survival of mice bearing E.G7-OVA tumors. The modularity of the SNA structure allows additional antigens to be readily incorporated into optimized nanostructures, yet the role of SNA anchor chemistry on the immunogenicity of clinically relevant cancer antigens remains unexplored. Given the impact of SNA structural designs on enhancing immunogenicity, $(C12)_9$-anchored SNAs could potentially open an avenue toward more successful translational outcomes when incorporating clinically relevant antigens, such as the HPV $E7_{11-19}$ peptide.

In this study, we explored the potential of employing $(C12)_9$-anchored SNAs, designed to include the HPV $E7_{11-19}$ peptide antigen, as a therapeutic approach for HPV-associated cancer. Our study involved a comparative analysis of similar treatments utilizing admix and SNAs made from the weaker anchoring cholesterol moiety or stronger $(C12)_9$ anchor. The central hypothesis examined was whether the more stable SNA construct would lead to a more effective therapeutic outcome. Our findings show robust cytotoxic $CD8^+$ T cell immunological responses raised by $(C12)_9$ E7 SNAs which incorporate the $E7_{11-19}$ peptide in an AAD transgenic mouse model. These responses include significant levels of effector memory $CD8^+$ T cells which secrete IFN-γ, an effector cytokine of antitumor immunity, and the generation of antigen-specific $CD8^+$ T cells cytotoxic against $E7_{11-19}$ presenting T2 cells. Building on previous findings that revealed the high stability (relative to cholesterol) of $(C12)_9$-SNAs in physiological conditions,[22] the biodistribution profile of $(C12)_9$-SNAs revealed high accumulation of immunostimulatory CpG DNA in lymph nodes driving the robust immune responses of $(C12)_9$-SNA observed *in vivo*. Furthermore, we present the translation of the antitumor immunity observed in the mouse model to clinically relevant human cell lines, such as human peripheral blood mononuclear cells (hPBMCs) and an HPV^+ HLA-A^*02^+ head and neck cancer model cell (UM-SCC-104). Toward this goal, our study reveals a higher degree of uptake and activation of human dendritic cells along with enhanced cytotoxicity of $CD8^+$ T cells against UM-SCC-104. Compared to a simple mixture of the vaccine components, termed admix, and cholesterol anchored SNAs, T cells raised by $(C12)_9$ E7 SNAs are more potent and demonstrate a superior ability to orchestrate an effective immune response in all measures. These findings highlight the potential of $(C12)_9$-SNAs as an effective structural vaccine which increases potency to a degree that can overcome the thus far underwhelming efficacy of HPV therapeutic vaccines.

The aqueous solubility of the $E7_{11-19}$ peptide facilitated SNA synthesis by encapsulating the peptide within the aqueous lumen of the liposomal SNA. Hydrating thin films of 1,2-

https://doi.org/10.1021/acs.nanolett.4c01392
Nano Lett. 2024, 24, 7629−7636

dioleoyl-*sn*-glycero-3-phosphocholine (DOPC) lipid with peptide dissolved in dulbecco's phosphate buffered saline (DPBS) produced liposomes containing between a 60 and 100 molar ratio of $E7_{11-19}$ peptides per liposome depending on the amount of peptide added to the thin film, matching the encapsulation efficiency of previously studied peptides.[16,22] The weighted average of peptides per liposome was a constant 75 for all experiments to minimize variability. These liposomes were then functionalized with the molar ratio of 75 $(C12)_9$ anchored or cholesterol anchored CpG oligonucleotides to synthesize SNAs encapsulating $E7_{11-19}$ peptide. The attachment of DNA to the liposomes was confirmed by dynamic light scattering (DLS), zeta-potential, and agarose gel electrophoresis (Figures S1 and S2). In addition, the cryo-electron microscopy images of E7 liposome, cholesterol E7 SNA, and $(C12)_9$ SNA did not exhibit significant morphological differences among the three samples (Figure S3). Moreover, the size distribution of E7 liposome, cholesterol E7 SNA, and $(C12)_9$ E7 SNA aligns with the DLS size measurements (Figure S1). Taken together, these data indicate the successful formulation of cholesterol E7 SNA and $(C12)_9$ E7 SNAs. Successful E7 SNA synthesis allows us to test whether structuring these components at the nanoscale can enhance the efficacy of therapeutic vaccines for HPV-associated cancers.

The *in vivo* efficacy of SNAs containing the $E7_{11-19}$ antigen was tested in AAD transgenic mice capable of recognizing peptide antigens with binding affinity for human HLA-A*02. These mice express a hybrid major histocompatibility complex (MHC) molecule containing the extracellular α-1 and α-2 domains of the human HLA-A*02 receptor and the transmembrane and cytoplasmic domains of murine H-$2D^d$.[23] We used the subcutaneous route for vaccination because it facilitates high accumulation of nanoparticles in the lymph nodes and enables prolonged release of vaccine cargo, thereby enhancing immune responses.[24,25] Additionally, our previous studies observed the sufficient induction of T-cell response using this route.[13,22,26,27] The mice were vaccinated every 2 weeks for three total injections with 6 nmol CpG 1826 (a murine TLR9 agonist) oligonucleotide and $E7_{11-19}$ peptide in the form of either an additive simple mixture in PBS (E7 Admix), or a liposomal SNA encapsulating the peptide antigen and functionalized with CpG DNA containing a 3′ hydrophobic cholesterol or $(C12)_9$ anchor (Figure 1A).

One week following the third vaccination (d 35), spleens were isolated from individual mice and tested for antigen specificity and phenotype of the $CD8^+$ T cell population. As our SNAs utilize an $E7_{11-19}$ antigen to target the HLA-A*02:01 MHC I allele, this antigen will be recognized by $CD8^+$ T cells. Therefore, our primary focus was to evaluate the functionality of memory $CD8^+$ T cells. To quantify the robustness of the immune response, the effector memory $CD8^+$ T cell population was quantified via flow cytometry by measuring the percentage of $CD8^+$ T cells in the spleen expressing $CD44^+CD62L^-$ surface markers (Figure 1B).[28] The mice treated with $(C12)_9$ E7 SNAs produced elevated level of effector T cells, resulting in a more than 2-fold increase in frequency of the $CD44^+CD62L^-$ phenotype in the $CD8^+$ T cell population compared to mice treated with admix. The antigen specificity of these T cells was assessed by measuring the production of IFN-γ via flow cytometry (Figure 1C) and an enzyme-linked immunosorbent spot (ELISpot) assay (Figures 1D and S4) following restimulation of the splenocytes with the $E7_{11-19}$ peptide. We also quantified CD107a surface expression to detect the effector $CD8^+$ T cells with their cytolytic functionality, since $CD107a^+IFN\text{-}\gamma^+$ T cells have been correlated with successful tumor inhibition.[29] Once more the $(C12)_9$ E7 SNA promoted the strongest antigen-specific immune response resulting in a 28-fold increase in the frequency of $CD8^+$ splenocytes double positive for both IFN-γ and CD107a compared to the admix-treated group. Other treatments failed to raise a significant quantity of cells positive for both IFN-γ and CD107a compared to the naive mice. The ELISpot measurements further corroborate these results; while the E7 admix did not produce any IFN-γ secreting spot-forming cells (SFCs), splenocytes from the $(C12)_9$ E7 SNA produced an average of 278 spot-forming cells (SFCs), an 8-fold enhancement compared to the cholesterol E7 SNA vaccine. The remaining splenocytes from the vaccinated mice were pooled together and the $CD8^+$ T cells were isolated by positive selection for each treatment condition. The cytotoxicity of these $CD8^+$ T cells was then tested by a 24 h coculture with $E7_{11-19}$ pulsed T2 cells, which are commonly used to assess HLA-A*02-specific T cell interactions (Figures 1E and S5).[30] The T cells raised from $(C12)_9$ E7 SNA vaccination were the only ones to exhibit significant killing of the target cell population, with ∼46% of the target cells being positive for both the early apoptosis marker Annexin V and the late apoptosis marker 7-AAD. The T cells raised from $(C12)_9$ E7 SNA vaccination were more than twice as cytotoxic compared to T cells raised from any other vaccination conditions. Together, these results exhibit the superior ability of $(C12)_9$ E7 SNA structures to promote powerful antigen-specific T cell responses *in vivo*.

To investigate whether the biodistribution of vaccine components correlate with the efficacy of SNA vaccines, we characterized the biodistribution profile of Cy5-labeled linear CpG or the SNA containing either a $(C12)_9$ or cholesterol anchor using an *in vivo* imaging system (IVIS) 24 h after subcutaneous administration. Overall, the greatest quantity of Cy5 signal was observed in the inguinal lymph nodes and liver (Figure 2A), which is expected since a subcutaneous administration accumulates in the inguinal lymph nodes and the liver often sequesters large macromolecules.[14,31] As the primary location for T-cell priming to generate an adaptive immune response, lymph nodes have been a key tissue for targeting therapeutic vaccines. Nanomaterials with a diameter of 10−100 nm are often considered the optimal size range for lymphatic drainage.[32−34] Due to their nanoscale structure, SNAs deliver their immunotherapeutic cargo more effectively to the lymph node. Specifically, when compared to the linear CpG oligonucleotide or cholesterol-SNA, the $(C12)_9$-SNA displayed a 2.4-fold or 1.3-fold increase in Cy5 signal, respectively (Figure 2A and B). To confirm these results, we isolated the lymphocytes in a single cell suspension and measured the degree of Cy5 labeled CpG DNA uptake across the entire lymphocyte population (Figure 2C). We observed Cy5 signal in over 44% of lymphocytes following vaccination, a 3.2-fold or 2-fold enhancement compared to linear CpG or the cholesterol SNA, respectively. Additionally, consistent with previous findings,[35] a significant amount of linear CpG accumulated in the kidney indicating that more of the linear oligonucleotide gets excreted 24 h after treatment likely due to its small size and difference in *in vivo* degradation kinetics (Figure 2A). No significant accumulation was observed in the other major organs examined. Collectively, these results show the superior ability of the $(C12)_9$ SNA structure to be

https://doi.org/10.1021/acs.nanolett.4c01392
Nano Lett. 2024, 24, 7629−7636

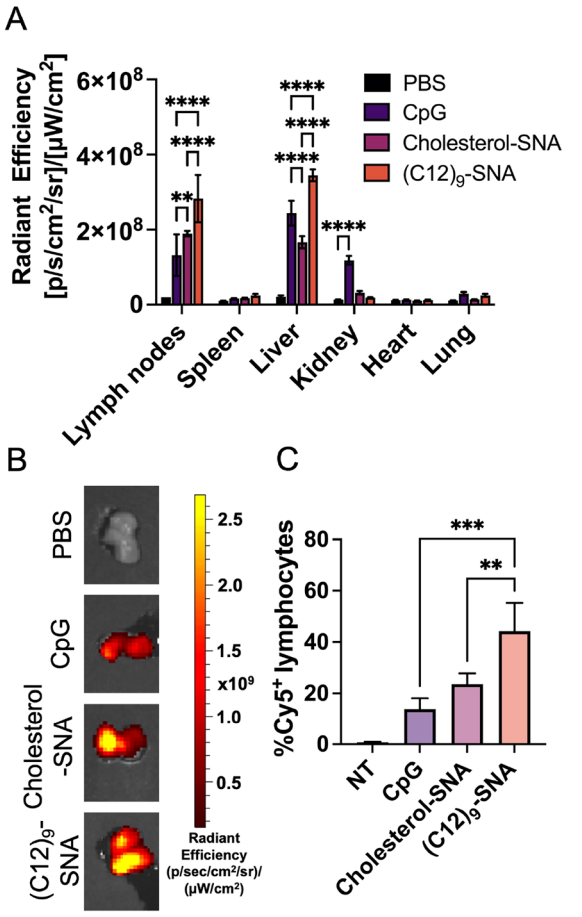

Figure 2. Biodistribution of Cy5-labeled DNA in mice after 24 h of subcutaneous injection. A. Calculated radiant efficiency of Cy5-labeled DNA (PBS, CpG, Cholesterol SNA, and $(C12)_9$-SNA) in whole organs (Lymph nodes, Spleen, Liver, Kidney, Heart, and Lung). B. Representative IVIS image of draining lymph nodes. C. Flow analysis of cellular distribution of Cy5-labeled DNA in draining lymph nodes. Data represents mean ± standard deviation. $n = 4$; statistical significance was calculated by one-way ANOVA with Tukey's post hoc test; $^*P < 0.05$, $^{**}P < 0.01$, $^{***}P < 0.005$, and $^{****}P < 0.001$.

efficiently delivered to the lymph node compared to linear CpG DNA and cholesterol-SNAs, supporting the enhancements in *in vivo* efficacy observed for the $(C12)_9$ E7 SNA.

Subsequently, we assessed the activation status of DCs in the draining lymph nodes (dLNs), hypothesizing that the enhanced accumulation of $(C12)_9$ SNAs in dLNs would result in increased expression of costimulatory markers. We aimed to detect the expression levels of costimulatory markers CD80 and CD86 specifically in $CD11c^+$ DCs in single cell suspension of lymphocytes using flow cytometry 24 h following subcutaneous injection of PBS, E7 Admix, cholesterol E7 SNA, or $(C12)_9$ E7 SNA. The expression levels of costimulatory molecules such as CD80 and CD86 on DCs are critical factors influencing the strength of the antitumor cytotoxic T lymphocyte response. We observed that codelivering CpG and antigen via SNAs were associated with approximately a 2-fold increase in the percentage of $CD11c^+$ DCs in lymphocytes, compared to mice treated with the admix control (Figure 3A). Additionally, we showed significant enhancement in the expression levels of costimulatory molecules CD80 and CD86 following SNA treatment (Figure

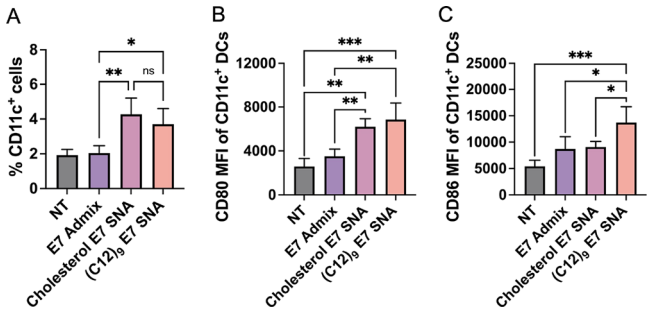

Figure 3. *In vivo* activation of dendritic cells (DCs) in the draining lymph nodes (dLNs) of AAD mice following treatment with E7 SNAs. AAD mice received subcutaneous administration of E7 admix, Cholesterol E7 SNA, or $(C12)_9$ E7 SNA. After 24 h, dLNs were harvested to assess dendritic cell activation. A. The percentage of $CD11c^+$ DCs in dLNs and the median fluorescent intensity of costimulatory molecules CD80 (B) and CD86 (C) expressed on these DCs were determined using flow cytometry. Data are presented as mean ± standard deviation ($n = 4$). Statistical significance was determined by one-way ANOVA with Tukey's post hoc test; $^*P < 0.05$, $^{**}P < 0.01$, $^{***}P < 0.005$, and $^{****}P < 0.001$.

3B and C). Generally, CD86 expression on DCs is abundant and rapidly upregulated compared to CD80.[36] However, $(C12)_9$ E7 SNAs resulted in a notably elevated expression of CD86 on DCs (MFI = 13,700 ± 3,000), in contrast to PBS (MFI = 5,400 ± 1,100), E7 Admix (MFI = 8,700 ± 2,300), and cholesterol E7 SNA (MFI = 9,000 ± 1,000) treatments. These findings highlight the enhanced ability of the $(C12)_9$ E7 SNA architecture to activate DCs within the lymph nodes when compared to simple mixture and cholesterol E7 SNAs. Moreover, they provide further validation for the improvements in *in vivo* efficacy noted with the inclusion of $(C12)_9$ E7 SNA.

We also measured the systemic secretion of proinflammatory cytokines (IL-6, IL-4, IL-1β, IL-12p70, IFN-γ, IL-10, IL-2, and TNF-α) in serum 24 h following treatment to evaluate the acute immune response generated by the vaccines. Prior work evaluated the immune response briefly (1 h) after vaccination finding that linear CpG led to rapid cytokine release compared to cholesterol SNA and $(C12)_9$ SNA treatments.[22] We report here a lower general degree of cytokine release at 24 h compared to 1 h. The linear CpG treatment results in a higher degree of proinflammatory cytokine secretion. While no significant difference in cytokine concentrations compared to untreated (NT) mice are observed for IFN-γ, IL-10, IL-2, and TNF-α regardless of treatment, linear CpG treatment led to a significantly greater degree of serum accumulation for the cytokines IL-6, IL-1β, and IL-12p70 compared to the NT control (Figure S7). Interestingly, the $(C12)_9$ SNA treatment led to significantly greater IL-4 secretion compared to both the NT control and cholesterol SNA. This evaluation of the acute immune response following vaccination reveals that the untargeted systemic secretion of cytokines into the bloodstream does not necessarily correlate with vaccine efficacy and can be explained by the unfavorable biodistribution profile of linear CpG which targets the lymph node less effectively, potentially leading to systemic inflammation and upregulation of pathways which inhibit antitumor immune responses such as checkpoint expression.

Due to the enhanced $E7_{11-19}$-specific cytotoxic T cell responses raised from AAD mice vaccinated with the $(C12)_9$ E7 SNAs, we expected that $(C12)_9$-SNAs with $E7_{11-19}$ antigen

https://doi.org/10.1021/acs.nanolett.4c01392
Nano Lett. 2024, 24, 7629−7636

and a human TLR-9 agonist (i.e., hCpG 7909) would result in the robust activation of human DCs. We assessed the ability of these SNAs, referred to as hSNAs, to stimulate the uptake and activation of primary human DCs within a population of hPBMCs, leading to the generation of antigen-specific cytotoxic T cells. As previously reported, SNA constructs have improved cellular uptake through a caveolae-mediated endocytic pathway using class A scavenger receptors.[17,37,38] The uptake of $(C12)_9$ hSNAs, cholesterol hSNAs, or liposomes labeled with a 1 mol % rhodamine dye lipid after a 4h incubation with hPBMCs was measured to confirm the ability of SNAs to enter primary human immune cells. We found a significantly higher internalization of $(C12)_9$ hSNAs (MFI = 12760 ± 1132, 33% liposome$^+$) into CD11c$^+$ DCs within the hPBMC population as compared to the liposome (MFI = 40 ± 1, 0% liposome$^+$) and cholesterol hSNAs (MFI = 3326 ± 52, 28% liposome$^+$) (Figure 4A and S8A). This trend is consistent

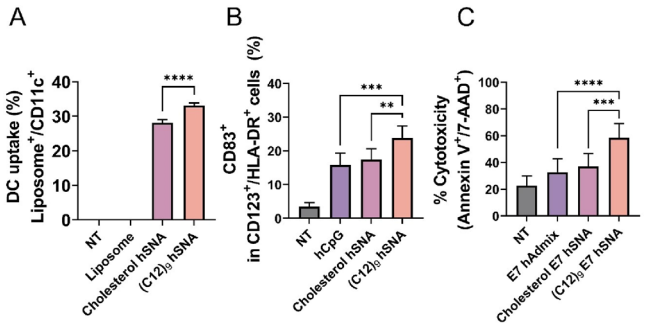

Figure 4. Activation of human PBMCs with SNAs. A. Median fluorescent intensity for CD11c$^+$ dendritic cellular uptake of SNAs. Human PBMC was treated with rhodamine labeled liposome, Cholesterol hSNA, and $(C12)_9$ hSNA for 4 h. B. Activation of plasmacytoid dendritic cells (pDCs, CD123$^+$). Costimulatory marker (CD83$^+$) was quantified after 24 h incubation with hCpG, Cholesterol hSNA and $(C12)_9$ hSNA. C. CD8$^+$ T cells responses against human UM-SCC-104 cells. CD8+ T cells are raised from incubation of human PBMCs with E7 hAdmix (CpG+E7$_{11-19}$), or E7$_{11-19}$ incorporated Cholesterol hSNA or $(C12)_9$ hSNA for 48 h. Cytotoxicity includes both apoptosis and necrosis, which are determined using Annexin V and 7-aminoactinomycin D (7-AAD) stain after 24 h coculture of CD8$^+$ T cells and UM-SCC-104 cells (25:1). Data represents mean ± standard deviation with n = 4−9; statistical significance was calculated by one-way ANOVA with Tukey's post hoc test; *P < 0.05, **P < 0.01, ***P < 0.005, and ****P < 0.001.

with the uptake measurement at 1 h where $(C12)_9$ hSNAs were internalized by 17% of DCs in hPBMCs (MFI = 6298 ± 1016) compared to liposomes by 0% of DCs in hPBMCs (MFI = 42 ± 4) and cholesterol hSNAs by 15% of DCs in hPBMCs (MFI = 2538 ± 308) (Figure S8B and C). The $(C12)_9$ anchored SNAs demonstrate the largest degree of uptake in human DCs due to their known high stability in physiological conditions.[22]

We next measured the activation of the dendritic cell population hypothesizing that the superior uptake and stability of the $(C12)_9$ hSNAs would lead to greater costimulatory marker expression. The activation of HLA-DR$^+$ DCs following 24 h of treatment with PBS, hCpG 7909, cholesterol hSNA, or $(C12)_9$ hSNA was measured by flow cytometry to detect the expression of costimulatory marker CD83 in CD123$^+$ plasmacytoid dendritic cells (pDCs) among HLA-A2$^+$ hPBMCs. pDCs are a major class of APC that produce type I interferons (IFNs) and induce the maturation of conventional dendritic cells (cDCs) for antiviral and antitumor immune responses.[39,40] However, in various cancer types, pDCs often persist in an immature state due to the presence of cytokines (e.g., VEGF, TNF-α, TGF-β, and IL-10) in the tumor microenvironment.[41] This lack of maturation and subsequent inactivation of pDCs lead to reduced type I interferon production, thereby promoting immunosuppression and tumor growth. Thus, activating pDCs is a crucial process to promoting antitumor immunity. The activation of pDCs was assessed via the expression of costimulatory marker CD83, which transports to the cellular surface from golgi and recycling endosome pools in DCs in response to TLR engagement.[42] As expected, $(C12)_9$ hSNAs induced a significantly higher percentage of CD83$^+$ pDCs (24%), compared to PBS (3%), hCpG 7909 (16%), and cholesterol hSNA (17%) treatment (Figure 4B). Given the consistent structural localization of the E7$_{11-19}$ antigen in the core of both cholesterol E7 hSNA and $(C12)_9$ E7 hSNA, we anticipate that the antigen processing pathways on dendritic cells would be similar between the two formulations, leading to comparable antigen presentation. Similar to a previous report,[17] the overall CD83 expression was increased in the presence of E7$_{11-19}$ antigen due to the antigen capture in pDCs.[43] Specifically, the same trend was observed where the mean percentage of the pDC populations expressing CD83 is 3%, 25%, 41% and 55% for the PBS, E7 hAdmix (hCpG + E7$_{11-19}$), cholesterol E7 hSNA and $(C12)_9$ E7 hSNA, respectively (Figure S9). Together, these results demonstrate the superior ability of $(C12)_9$ hSNA structures to both internalize and potently activate human APCs.

Next, to evaluate antitumor effects of antigen-specific cytotoxic T cells raised from different treatments; PBS, E7 hAdmix, cholesterol E7 hSNAs, and $(C12)_9$ E7 hSNAs were applied to HLA-A*02$^+$ hPBMCs. CD8$^+$ T cells from the treated hPBMCs were then purified and cocultured for 24 h with a clinically relevant HPV$^+$ cancer cell line, UM-SCC-104.[44] The cytotoxic effect of the T cells against this cell line was determined using a flow analysis to detect early apoptotic (Annexin V$^+$) and necrotic (7-aminoactinomycin D$^+$) cells. We found that CD8$^+$ T cells raised from hPBMCs treated with $(C12)_9$ E7 hSNAs (60%) improved cancer cell killing significantly compared to PBS (23%), E7 Admix (33%), and cholesterol E7 hSNAs (37%) (Figure 4C). Specifically, CD8$^+$ T cells raised from hPBMCs treated with $(C12)_9$ E7 hSNA resulted in approximately 2-fold or 1.5-fold higher cytotoxicity of UM-SCC-104, as compared to the E7 Admix or cholesterol E7 hSNA, respectively. These findings show that $(C12)_9$-hSNA constructs enhance the immunogenicity of an HLA-A*02 restricted antigen, previously unsuccessful in vaccine clinical trials, resulting in more potent antigen-specific cytotoxic T cells immune responses against an HPV-associated cancer cell line. Taken together, these data highlight the clinical translational potential of the SNA, and how tailoring the chemical and structural changes of SNAs can affect the biological functions of cargo.

The work described here underscores the importance of cancer vaccine structure, in addition to components, in dictating efficacy. Indeed, a well-optimized SNA structure containing the clinically relevant E7$_{11-19}$ peptide antigen generates much greater antigen-specific T cell responses in both humanized mice and human cells than the unstructured components or analogous structures made with a cholesterol

https://doi.org/10.1021/acs.nanolett.4c01392
Nano Lett. 2024, 24, 7629−7636

anchor. Simply changing a seemingly minor parameter (i.e., the anchor chemistry) of the SNA vaccine shifts the immune response from one that is mostly ineffective to highly potent. This finding holds broad implications for therapeutic vaccine design, emphasizing the critical role of the structural arrangement of vaccine components in developing the most efficacious vaccines. More importantly in the context of cancer vaccines, the use of ineffective structures may be the primary cause of poor clinical efficacy, as opposed to the choice of specific vaccine components.

■ ASSOCIATED CONTENT

Supporting Information

The Supporting Information is available free of charge at https://pubs.acs.org/doi/10.1021/acs.nanolett.4c01392.

Materials and methods, DNA sequences used in this study, dynamic light scattering intensity means, zeta potential, gel electrophoresis of SNAs, Cryo-EM of SNAs, $E7_{11-19}$ specific T cell killing with different effector to target ratio, representative biodistribution IVIS image, the average radiant efficiency ratio of lymph node to liver, the levels of proinflammatory cytokines in serum after SNA treatments, representative IFN-γ ELISpot image, human dendritic cell uptake of SNAs after 1 h, and human dendritic cell activation after 24 h of SNA containing $E7_{11-19}$ treatment (PDF)

■ AUTHOR INFORMATION

Corresponding Authors

Jochen Lorch − *Department of Medicine, Hematology/Oncology Division, Robert H. Lurie Comprehensive Cancer Center, Feinberg School of Medicine, Northwestern University, Chicago, Illinois 60611, United States*; Email: jochen.lorch@nm.org

Chad A. Mirkin − *Department of Chemistry and International Institute for Nanotechnology and Department of Biomedical Engineering, Northwestern University, Evanston, Illinois 60208, United States*; orcid.org/0000-0002-6634-7627; Email: chadnano@northwestern.edu

Authors

Jeongmin Hwang − *Department of Chemistry and International Institute for Nanotechnology, Northwestern University, Evanston, Illinois 60208, United States*

Jasper Wilson Dittmar − *Department of Biomedical Engineering, Northwestern University, Evanston, Illinois 60208, United States*

Janice Kang − *Department of Chemistry and International Institute for Nanotechnology, Northwestern University, Evanston, Illinois 60208, United States*

Tonatiuh Ocampo − *Department of Interdisciplinary Biological Sciences, Northwestern University, Evanston, Illinois 60208, United States*

Michael Evangelopoulos − *Department of Biomedical Engineering, Northwestern University, Evanston, Illinois 60208, United States*; orcid.org/0000-0002-5300-4289

Zhenyu Han − *Department of Chemistry and International Institute for Nanotechnology, Northwestern University, Evanston, Illinois 60208, United States*; orcid.org/0000-0003-3798-9345

Sergej Kudruk − *Department of Chemistry and International Institute for Nanotechnology, Northwestern University, Evanston, Illinois 60208, United States*

Complete contact information is available at: https://pubs.acs.org/10.1021/acs.nanolett.4c01392

Author Contributions

‖J.H. and J.W.D. contributed equally to this work.

Notes

The content is solely the responsibility of the authors and does not necessarily represent the official views of the National Institutes of Health or Northwestern University.

The authors declare the following competing financial interest(s): C.A.M. has financial interest in Flashpoint Therapeutics Inc., which could potentially benefit from the outcomes of this research.

■ ACKNOWLEDGMENTS

Research reported in this publication was supported by the National Cancer Institute of the National Institutes of Health under Award Number R01CA257926, P50CA221747, and R01CA275430. This work was also supported by the Air Force Office of Scientific Research award FA9550-22-1-0300 and the National Science Foundation grant DMR-2104353. J.H. acknowledges support from Robert H. Lurie Cancer Center's Translation Bridge Training Program at Northwestern University supported through generous philanthropy. J.D. was partially supported by a fellowship associated with the Chemistry of Life Processes Predoctoral Training Program at Northwestern University. T.O. was partially supported by a fellowship associated with the Biotechnology Training Program at Northwestern University. M.E. was partially supported by the Dr. John N. Nicholson Fellowship and the Alexander S. Onassis Public Benefit Foundation. This work made use of the IMSERC MS facility at Northwestern University, which has received support from the Soft and Hybrid Nanotechnology Experimental (SHyNE) Resource (NSF ECCS-2025633), the State of Illinois, and the International Institute for Nanotechnology (IIN). Imaging work was performed at the Northwestern University Center for Advanced Molecular Imaging (RRID:SCR_021192) generously supported by NCI CCSG P30 CA060553 awarded to the Robert H Lurie Comprehensive Cancer Center. Cryo-TEM imaging work made use of the BioCryo facility of Northwestern University's NUANCE Center, which has received support from the SHyNE Resource (NSF ECCS-2025633), the IIN, and Northwestern's MRSEC program (NSF DMR-2308691). Finally, we acknowledge the Immunotherapy assessment core at the Robert H Lurie Comprehensive Cancer Center of Northwestern University, especially Dr. Surya Pandey and Li Kai for their assistance in serum cytokine analysis.

■ ABBREVIATIONS

SNA, spherical nucleic acid; HPV, human papillomavirus; TLR, Toll-like receptor; DNA, DNA; HLA-A*02, human leukocyte antigen serotype A2; hPBMCs, human peripheral blood mononuclear cells; DOPC, 1,2-dioleoyl-*sn*-glycero-3-phosphocholine; DPBS, Dulbecco's phosphate buffered saline

■ REFERENCES

(1) Liao, C.; Francoeur, A. A.; Kapp, D. S.; Caesar, M. A. P.; Huh, W. K.; Chan, J. K. Trends in Human Papillomavirus-Associated

Cancers, Demographic Characteristics, and Vaccinations in the US, 2001−2017. *JAMA network open* **2022**, *5* (3), e222530.
(2) Gribb, J. P.; Wheelock, J. H.; Park, E. S. Human Papilloma Virus (HPV) and the Current State of Oropharyngeal Cancer Prevention and Treatment. *Dela J. Public Health* **2023**, *9* (1), 26−28.
(3) Vats, A.; Trejo-Cerro, O.; Thomas, M.; Banks, L. Human papillomavirus E6 and E7: What remains? *Tumour Virus Res.* **2021**, *11*, 200213.
(4) Nagarsheth, N. B.; Norberg, S. M.; Sinkoe, A. L.; Adhikary, S.; Meyer, T. J.; Lack, J. B.; Warner, A. C.; Schweitzer, C.; Doran, S. L.; Korrapati, S.; Stevanović, S.; Trimble, C. L.; Kanakry, J. A.; Bagheri, M. H.; Ferraro, E.; Astrow, S. H.; Bot, A.; Faquin, W. C.; Stroncek, D.; Gkitsas, N.; Highfill, S.; Hinrichs, C. S. TCR-engineered T cells targeting E7 for patients with metastatic HPV-associated epithelial cancers. *Nature medicine* **2021**, *27* (3), 419−425.
(5) Baulu, E.; Gardet, C.; Chuvin, N.; Depil, S. TCR-engineered T cell therapy in solid tumors: State of the art and perspectives. *Sci. Adv.* **2023**, *9* (7), No. eadf3700.
(6) Riemer, A. B.; Keskin, D. B.; Zhang, G.; Handley, M.; Anderson, K. S.; Brusic, V.; Reinhold, B.; Reinherz, E. L. A conserved E7-derived cytotoxic T lymphocyte epitope expressed on human papillomavirus 16-transformed HLA-A2+ epithelial cancers. *J. Biol. Chem.* **2010**, *285* (38), 29608−22.
(7) ClinicalTrials.gov, Trial To Test Safety And Efficacy Of Vaccination For Incurable HPV 16-Related Oropharyngeal, Cervical And Anal Cancer. https://clinicaltrials.gov/study/NCT02865135 (accessed 01/08/2024).
(8) Cutler, J. I.; Auyeung, E.; Mirkin, C. A. Spherical nucleic acids. *J. Am. Chem. Soc.* **2012**, *134* (3), 1376−91.
(9) Liu, S.; Yu, C. Y.; Wei, H. Spherical nucleic acids-based nanoplatforms for tumor precision medicine and immunotherapy. *Materials today. Bio* **2023**, *22*, 100750.
(10) Huang, Z.; Callmann, C. E.; Wang, S.; Vasher, M. K.; Evangelopoulos, M.; Petrosko, S. H.; Mirkin, C. A. Rational Vaccinology: Harnessing Nanoscale Chemical Design for Cancer Immunotherapy. *ACS central science* **2022**, *8* (6), 692−704.
(11) Kumthekar, P.; Ko, C. H.; Paunesku, T.; Dixit, K.; Sonabend, A. M.; Bloch, O.; Tate, M.; Schwartz, M.; Zuckerman, L.; Lezon, R.; Lukas, R. V.; Jovanovic, B.; McCortney, K.; Colman, H.; Chen, S.; Lai, B.; Antipova, O.; Deng, J.; Li, L.; Tommasini-Ghelfi, S.; Hurley, L. A.; Unruh, D.; Sharma, N. V.; Kandpal, M.; Kouri, F. M.; Davuluri, R. V.; Brat, D. J.; Muzzio, M.; Glass, M.; Vijayakumar, V.; Heidel, J.; Giles, F. J.; Adams, A. K.; James, C. D.; Woloschak, G. E.; Horbinski, C.; Stegh, A. H. A first-in-human phase 0 clinical study of RNA interference-based spherical nucleic acids in patients with recurrent glioblastoma. *Sci. Transl Med.* **2021**, *13* (584), No. eabb3945.
(12) Daniel, W. L.; Lorch, U.; Mix, S.; Bexon, A. S. A first-in-human phase 1 study of cavrotolimod, a TLR9 agonist spherical nucleic acid, in healthy participants: Evidence of immune activation. *Front. Immunol.* **2022**, *13*, 1073777.
(13) Qin, L.; Wang, S.; Dominguez, D.; Long, A.; Chen, S.; Fan, J.; Ahn, J.; Skakuj, K.; Huang, Z.; Lee, A.; Mirkin, C.; Zhang, B. Development of Spherical Nucleic Acids for Prostate Cancer Immunotherapy. *Front. Immunol.* **2020**, *11*, 1333.
(14) Teplensky, M.; Evangelopoulos, M.; Dittmar, J.; Forsyth, C.; Sinegra, A.; Wang, S.; Mirkin, C. Multi-antigen spherical nucleic acid cancer vaccines. *Nature biomedical engineering* **2023**, *7* (7), 911−927.
(15) Radovic-Moreno, A. F.; Chernyak, N.; Mader, C. C.; Nallagatla, S.; Kang, R. S.; Hao, L. L.; Walker, D. A.; Halo, T. L.; Merkel, T. J.; Rische, C. H.; Anantatmula, S.; Burkhart, M.; Mirkin, C. A.; Gryaznov, S. M. Immunomodulatory spherical nucleic acids. *P Natl. Acad. Sci. USA* **2015**, *112* (13), 3892−3897.
(16) Wang, S.; Qin, L.; Yamankurt, G.; Skakuj, K.; Huang, Z.; Chen, P. C.; Dominguez, D.; Lee, A.; Zhang, B.; Mirkin, C. A. Rational vaccinology with spherical nucleic acids. *Proc. Natl. Acad. Sci. U.S.A.* **2019**, *116* (21), 10473−10481.
(17) Teplensky, M. H.; Dittmar, J. W.; Qin, L.; Wang, S.; Evangelopoulos, M.; Zhang, B.; Mirkin, C. A. Spherical Nucleic Acid Vaccine Structure Markedly Influences Adaptive Immune Responses of Clinically Utilized Prostate Cancer Targets. *Adv. Healthcare Mater.* **2021**, *10* (22), No. e2101262.
(18) Skakuj, K.; Wang, S.; Qin, L.; Lee, A.; Zhang, B.; Mirkin, C. A. Conjugation Chemistry-Dependent T-Cell Activation with Spherical Nucleic Acids. *J. Am. Chem. Soc.* **2018**, *140* (4), 1227−1230.
(19) Skakuj, K.; Teplensky, M. H.; Wang, S.; Dittmar, J. W.; Mirkin, C. A. Chemically Tuning the Antigen Release Kinetics from Spherical Nucleic Acids Maximizes Immune Stimulation. *ACS Cent. Sci.* **2021**, *7* (11), 1838−1846.
(20) Meckes, B.; Banga, R. J.; Nguyen, S. T.; Mirkin, C. A. Enhancing the Stability and Immunomodulatory Activity of Liposomal Spherical Nucleic Acids through Lipid-Tail DNA Modifications. *Small* **2018**, *14* (5), 1702909.
(21) Callmann, C. E.; Kusmierz, C. D.; Dittmar, J. W.; Broger, L.; Mirkin, C. A. Impact of Liposomal Spherical Nucleic Acid Structure on Immunotherapeutic Function. *ACS Cent Sci.* **2021**, *7* (5), 892−899.
(22) Dittmar, J. W.; Teplensky, M. H.; Evangelopoulos, M.; Qin, L.; Zhang, B.; Mirkin, C. A. Tuning DNA Dissociation from Spherical Nucleic Acids for Enhanced Immunostimulation. *ACS Nano* **2023**, *17* (18), 17996−18007.
(23) Newberg, M. H.; Smith, D. H.; Haertel, S. B.; Vining, D. R.; Lacy, E.; Engelhard, V. H. Importance of MHC class 1 alpha2 and alpha3 domains in the recognition of self and non-self MHC molecules. *Journal of immunology (Baltimore, Md.: 1950)* **1996**, *156* (7), 2473−80.
(24) Truex, N. L.; Rondon, A.; Rossler, S. L.; Hanna, C. C.; Cho, Y.; Wang, B. Y.; Backlund, C. M.; Lutz, E. A.; Irvine, D. J.; Pentelute, B. L. Enhanced Vaccine Immunogenicity Enabled by Targeted Cytosolic Delivery of Tumor Antigens into Dendritic Cells. *ACS Cent Sci.* **2023**, *9* (9), 1835−1845.
(25) Song, K.; Pun, S. H. Design and Evaluation of Synthetic Delivery Formulations for Peptide-Based Cancer Vaccines. *BME Front.* **2024**, *5*, No. 0038.
(26) Wang, S.; Qin, L.; Yamankurt, G.; Skakuj, K.; Huang, Z.; Chen, P. C.; Dominguez, D.; Lee, A.; Zhang, B.; Mirkin, C. A. Rational vaccinology with spherical nucleic acids. *Proc. Natl. Acad. Sci. U. S. A.* **2019**, *116* (21), 10473−10481.
(27) Teplensky, M. H.; Evangelopoulos, M.; Dittmar, J. W.; Forsyth, C. M.; Sinegra, A. J.; Wang, S.; Mirkin, C. A. Multi-antigen spherical nucleic acid cancer vaccines. *Nat. Biomed Eng.* **2023**, *7* (7), 911−927.
(28) Gerberick, G. F.; Cruse, L. W.; Miller, C. M.; Sikorski, E. E.; Ridder, G. M. Selective modulation of T cell memory markers CD62L and CD44 on murine draining lymph node cells following allergen and irritant treatment. *Toxicology and applied pharmacology* **1997**, *146* (1), 1−10.
(29) De Groot, R.; Van Loenen, M. M.; Guislain, A.; Nicolet, B. P.; Freen-Van Heeren, J. J.; Verhagen, O. J. H. M.; Van Den Heuvel, M. M.; De Jong, J.; Burger, P.; Van Der Schoot, C. E.; Spaapen, R. M.; Amsen, D.; Haanen, J. B. A. G.; Monkhorst, K.; Hartemink, K. J.; Wolkers, M. C. Polyfunctional tumor-reactive T cells are effectively expanded from non-small cell lung cancers, and correlate with an immune-engaged T cell profile. *Oncoimmunology* **2019**, *8* (11), No. e1648170.
(30) Weinzierl, A. O.; Rudolf, D.; Hillen, N.; Tenzer, S.; van Endert, P.; Schild, H.; Rammensee, H. G.; Stevanović, S. Features of TAP-independent MHC class I ligands revealed by quantitative mass spectrometry. *European journal of immunology* **2008**, *38* (6), 1503−10.
(31) Ferrer, J. R.; Sinegra, A. J.; Ivancic, D.; Yeap, X. Y.; Qiu, L.; Wang, J.-J.; Zhang, Z. J.; Wertheim, J. A.; Mirkin, C. A. Structure-Dependent Biodistribution of Liposomal Spherical Nucleic Acids. *ACS Nano* **2020**, *14* (2), 1682−1693.
(32) Gause, K. T.; Wheatley, A. K.; Cui, J.; Yan, Y.; Kent, S. J.; Caruso, F. Immunological Principles Guiding the Rational Design of Particles for Vaccine Delivery. *ACS Nano* **2017**, *11* (1), 54−68.
(33) Howard, G. P.; Verma, G.; Ke, X.; Thayer, W. M.; Hamerly, T.; Baxter, V. K.; Lee, J. E.; Dinglasan, R. R.; Mao, H.-Q. Critical size limit of biodegradable nanoparticles for enhanced lymph node

https://doi.org/10.1021/acs.nanolett.4c01392
Nano Lett. 2024, 24, 7629−7636

trafficking and paracortex penetration. *Nano Res.* **2019**, *12* (4), 837−844.
(34) McCright, J.; Naiknavare, R.; Yarmovsky, J.; Maisel, K. Targeting Lymphatics for Nanoparticle Drug Delivery. *Frontiers in pharmacology* **2022**, *13*, 887402.
(35) Ferrer, J. R.; Sinegra, A. J.; Ivancic, D.; Yeap, X. Y.; Qiu, L.; Wang, J. J.; Zhang, Z. J.; Wertheim, J. A.; Mirkin, C. A. Structure-Dependent Biodistribution of Liposomal Spherical Nucleic Acids. *ACS Nano* **2020**, *14* (2), 1682−1693.
(36) Sansom, D. M.; Manzotti, C. N.; Zheng, Y. What's the difference between CD80 and CD86? *Trends Immunol* **2003**, *24* (6), 313−319.
(37) Banga, R. J.; Chernyak, N.; Narayan, S. P.; Nguyen, S. T.; Mirkin, C. A. Liposomal Spherical Nucleic Acids. *J. Am. Chem. Soc.* **2014**, *136* (28), 9866−9869.
(38) Choi, C. H.; Hao, L.; Narayan, S. P.; Auyeung, E.; Mirkin, C. A. Mechanism for the endocytosis of spherical nucleic acid nanoparticle conjugates. *Proc. Natl. Acad. Sci. U. S. A.* **2013**, *110* (19), 7625−30.
(39) Del Prete, A.; Salvi, V.; Soriani, A.; Laffranchi, M.; Sozio, F.; Bosisio, D.; Sozzani, S. Dendritic cell subsets in cancer immunity and tumor antigen sensing. *Cellular & Molecular Immunology* **2023**, *20* (5), 432−447.
(40) Fu, C.; Peng, P.; Loschko, J.; Feng, L.; Pham, P.; Cui, W.; Lee, K. P.; Krug, A. B.; Jiang, A. Plasmacytoid dendritic cells cross-prime naive CD8 T cells by transferring antigen to conventional dendritic cells through exosomes. *P Natl. Acad. Sci. USA* **2020**, *117* (38), 23730−23741.
(41) Zhou, B.; Lawrence, T.; Liang, Y. The Role of Plasmacytoid Dendritic Cells in Cancers. *Frontiers in immunology* **2021**, *12*, 749190.
(42) Poropatich, K.; Dominguez, D.; Chan, W. C.; Andrade, J.; Zha, Y.; Wray, B.; Miska, J.; Qin, L.; Cole, L.; Coates, S.; Patel, U.; Samant, S.; Zhang, B. OX40+ plasmacytoid dendritic cells in the tumor microenvironment promote antitumor immunity. *J. Clin. Invest.* **2020**, *130* (7), 3528−3542.
(43) Arroyo Hornero, R.; Idoyaga, J. Plasmacytoid dendritic cells: A dendritic cell in disguise. *Molecular immunology* **2023**, *159*, 38−45.
(44) Tang, A. L.; Hauff, S. J.; Owen, J. H.; Graham, M. P.; Czerwinski, M. J.; Park, J. J.; Walline, H.; Papagerakis, S.; Stoerker, J.; McHugh, J. B.; Chepeha, D. B.; Bradford, C. R.; Carey, T. E.; Prince, M. E. UM-SCC-104: a new human papillomavirus-16-positive cancer stem cell-containing head and neck squamous cell carcinoma cell line. *Head & neck* **2012**, *34* (10), 1480−91.

https://doi.org/10.1021/acs.nanolett.4c01392
Nano Lett. 2024, 24, 7629−7636